

Semi-inclusive nonleptonic decays $B \rightarrow D_s^{(*)} X$

Changhao Jin

School of Physics, University of Melbourne, Victoria 3010, Australia

Abstract

We calculate the total and differential decay rates for the semi-inclusive nonleptonic decays $B \rightarrow D_s^{(*)} X_q$ ($q = c$ or u) under the factorization hypothesis. The initial bound state effect is treated using the light-cone expansion and the heavy quark effective theory. We investigate the contribution of the penguin amplitude for the decay mode $B \rightarrow D_s^{(*)} X_c$ and find that it is small but non-negligible. The resulting decay rates for $B \rightarrow D_s^{(*)} X_c$ agree with the measurements. The use of the decay mode $B \rightarrow D_s^{(*)} X_u$ to determine $|V_{ub}|$ is discussed.

I. INTRODUCTION

The semi-inclusive nonleptonic decays $B \rightarrow D_s^{(*)} X_q$ ($q = c$ or u), where X_q is a hadronic system containing a q -quark, can be used to study mechanisms of the production of the $D_s^{(*)}$ meson in B meson decays, as well as the dynamics of the strong interactions [1]. As pointed out in Ref. [2], the Cabibbo-Kobayashi-Maskawa (CKM) matrix element $|V_{ub}|$ can be determined by the measurement of the momentum spectrum of the $D_s^{(*)}$ meson in $B \rightarrow D_s^{(*)} X_u$. An advantage of the method¹ is that the majority of the spectrum in the rare decays $B \rightarrow D_s^{(*)} X_u$ lie above the kinematic limit for $B \rightarrow D_s^{(*)} X_c$ which constitutes an overwhelming background. Since this method involves nonleptonic B decays, in which only hadrons appear in the final state, the hadronic complications may be more sever than the determination of $|V_{ub}|$ from semileptonic decays $B \rightarrow \ell \bar{\nu}_\ell X_u$. An understanding of the strong interactions, which are responsible for the confinement of quarks and gluons in hadrons, in the weak decays is essential to a determination of $|V_{ub}|$.

Measurements of the branching fraction for $B \rightarrow D_s X$ have been reported by ARGUS and CLEO. The average of their results gives $\mathcal{B}(B \rightarrow D_s^\pm X) = (10.0 \pm 2.5)\%$ [4]. Recently, new precise measurements of D_s^+ and D_s^{*+} meson production from B meson decays have been presented by BABAR [5]. The results for the branching fractions are $\mathcal{B}(B \rightarrow D_s^+ X) = (10.93 \pm 0.19 \pm 0.58 \pm 2.73)\%$ and $\mathcal{B}(B \rightarrow D_s^{*+} X) = (7.9 \pm 0.8 \pm 0.7 \pm 2.0)\%$. As for the rare decays $B \rightarrow D_s^{(*)} X_u$, none of them have been experimentally measured. With high-statistics event sample from the B factories, coupled with improvements in detector performance and analysis techniques, measurements of $B \rightarrow D_s^{(*)} X_u$ might be possible in the near future.

The $b \rightarrow q \bar{c} s$ tree transition is expected to dominate $\bar{B} \rightarrow D_s^{(*)-} X_q$ decays. In these processes the b quark decays to a c or a u quark, emitting a virtual W that fragments to a $\bar{c} s$ quark pair that subsequently hadronizes into a $D_s^{(*)-}$ meson. The effective weak Hamiltonian responsible for the decays is well known [6], which is based on the operator product expansion [7] and the renormalization group [8]. The problem is how to calculate hadronic matrix elements of four-quark operators in the effective weak Hamiltonian. Factorization hypothesis has widely been used in calculations of nonleptonic B decays, which reduce the hadronic matrix element of a four-quark operator to the product of two matrix elements of current operators [9]. The argument for factorization is based on the space-time evolution of the decay products [10]. At the quark level the decay $\bar{B} \rightarrow D_s^{(*)-} X_q$ begins as a nearly collinear configuration of $b \rightarrow q + (\bar{c} s)$, with q and the $(\bar{c} s)$ pair moving rapidly apart in opposite directions. When the color singlet $D_s^{(*)-}$ meson is formed, it is far away from the hadronic system X_q recoiling against it. The strong interaction between them is expected to be not significant. Therefore, the hadronic matrix element can be factorized into a product of hadronic matrix elements of color-singlet quark currents. For $\bar{B} \rightarrow D_s^{(*)-} X_c$ due to limited energy release this argument is considered to be weaker than $\bar{B} \rightarrow D_s^{(*)-} X_u$. Factorization in the nonleptonic B decays with the emission particle being a light meson can be justified more rigorously in the heavy quark limit using perturbative QCD, where the emission particle means the one that does not inherit the spectator quark from the B meson [11–13].

¹Other methods of extracting $|V_{ub}|$ from nonleptonic B decays have also been proposed [3].

Unfortunately, this is not the case for both $\bar{B} \rightarrow D_s^{(*)-} X_c$ and $\bar{B} \rightarrow D_s^{(*)-} X_u$ decays, where the emission particle is $D_s^{(*)-}$ that is not light. Nevertheless, factorization has been found to hold with current accuracy in the color-favored decay modes $\bar{B}^0 \rightarrow D_s^{(*)-} D^{(*)+}$, where no perturbative QCD justification has been presented [14]. Thus, we have some confidence in the applicability of factorization to the color-favored decay modes $\bar{B} \rightarrow D_s^{(*)-} X_q$.

In this paper, we analyze $\bar{B} \rightarrow D_s^{(*)-} X_q$ decays in some detail. We shall calculate the total and differential $\bar{B} \rightarrow D_s^{(*)-} X_q$ decay rates assuming factorization. We include the contributions of penguin diagrams to $\bar{B} \rightarrow D_s^{(*)-} X_c$ decays, which turn out to be small but non-negligible. After factorization the long-distance QCD effects on $\bar{B} \rightarrow D_s^{(*)-} X_q$ decays are contained in two matrix elements: One is related to the decay constant for the $D_s^{(*)}$ meson, accounting for the direct generation of the $D_s^{(*)}$ meson from the vacuum by the $\bar{c}s$ current forming the weak Hamiltonian, while the other incorporates the effect of the initial b quark bound state in the B meson, which relates a b -quark decay to a B -meson decay. The treatment of the initial bound state effect will be the main focus of this paper. We shall use the light-cone expansion and the heavy quark effective theory (HQET) [15] to make our calculations aimed at understanding this effect from QCD.

II. FACTORIZATION

Both $\bar{B} \rightarrow D_s^{(*)-} X_c$ and $\bar{B} \rightarrow D_s^{(*)-} X_u$ involve tree amplitudes. In addition, penguin amplitudes contribute to $\bar{B} \rightarrow D_s^{(*)-} X_c$. The annihilation and exchange diagrams are estimated to give much smaller contributions than the tree diagram [2]. We shall neglect them. The relevant $\Delta B = 1$ effective Hamiltonian reads

$$\mathcal{H}_{\text{eff}} = \frac{G_F}{\sqrt{2}} \left\{ V_{qb} V_{cs}^* (c_1 O_1^q + c_2 O_2^q) - V_{tb} V_{ts}^* \sum_{n=3}^{10} c_n O_n \right\}, \quad (1)$$

where $O_{1,2}^q$ are the tree operators and O_{3-6} (O_{7-10}) the QCD (electroweak) penguin operators. They are given by

$$\begin{aligned} O_1^q &= (\bar{q}_i b_i)_{V-A} (\bar{s}_j c_j)_{V-A}, \quad O_2^q = (\bar{q}_i b_j)_{V-A} (\bar{s}_j c_i)_{V-A}, \\ O_{3(5)} &= (\bar{s}_i b_i)_{V-A} \sum_{q'} (\bar{q}'_j q'_j)_{V-(+)A}, \quad O_{4(6)} = (\bar{s}_i b_j)_{V-A} \sum_{q'} (\bar{q}'_j q'_i)_{V-(+)A}, \\ O_{7(9)} &= \frac{3}{2} (\bar{s}_i b_i)_{V-A} \sum_{q'} e_{q'} (\bar{q}'_j q'_j)_{V+(-)A}, \quad O_{8(10)} = \frac{3}{2} (\bar{s}_i b_j)_{V-A} \sum_{q'} e_{q'} (\bar{q}'_j q'_i)_{V+(-)A}, \end{aligned} \quad (2)$$

where i and j are color indices, $(\bar{q}_1 q_2)_{V\pm A} = \bar{q}_1 \gamma_\mu (1 \pm \gamma_5) q_2$, the summation runs over $q' = u, d, s, c, b$, and $e_{q'}$ is the electric charge of the q' quark in units of $|e|$.

The Wilson coefficients c_n have been calculated in different schemes [6]. In this paper we shall consistently use the naive dimensional regularization scheme. Including the next-to-leading order QCD corrections, the values of c_n at the renormalization scale m_b are [6]

$$\begin{aligned} c_1 &= 1.082, \quad c_2 = -0.185, \quad c_3 = 0.014, \quad c_4 = -0.035, \quad c_5 = 0.009, \quad c_6 = -0.041, \\ c_7 &= -0.002 \alpha_{em}, \quad c_8 = 0.054 \alpha_{em}, \quad c_9 = -1.292 \alpha_{em}, \quad c_{10} = 0.263 \alpha_{em}. \end{aligned}$$

Here $\alpha_{em} = 1/137$ is the electromagnetic fine structure constant.

Under the factorization hypothesis, we obtain from the effective Hamiltonian in Eq. (1) the decay amplitudes

$$A(\bar{B} \rightarrow D_s^- X_c) = i f_{D_s} \left(\alpha p_{D_s}^\mu \langle X_c | j_\mu^c | \bar{B} \rangle + \beta \langle X_c | J | \bar{B} \rangle \right), \quad (3)$$

$$A(\bar{B} \rightarrow D_s^{*-} X_c) = \alpha m_{D_s^*} f_{D_s^*} \epsilon^{\mu*} \langle X_c | j_\mu^c | \bar{B} \rangle, \quad (4)$$

$$A(\bar{B} \rightarrow D_s^- X_u) = i \frac{G_F}{\sqrt{2}} V_{ub} V_{cs}^* a_1 f_{D_s} p_{D_s}^\mu \langle X_u | j_\mu^u | \bar{B} \rangle, \quad (5)$$

$$A(\bar{B} \rightarrow D_s^{*-} X_u) = \frac{G_F}{\sqrt{2}} V_{ub} V_{cs}^* a_1 m_{D_s^*} f_{D_s^*} \epsilon^{\mu*} \langle X_u | j_\mu^u | \bar{B} \rangle, \quad (6)$$

where

$$\alpha = \frac{G_F}{\sqrt{2}} [V_{cb} V_{cs}^* a_1 - V_{tb} V_{ts}^* (a_4 + a_{10})], \quad (7)$$

$$\beta = \frac{G_F}{\sqrt{2}} V_{tb} V_{ts}^* (a_6 + a_8) \frac{2m_{D_s}^2}{m_c + m_s}, \quad (8)$$

$$a_{2i} = c_{2i} + \frac{c_{2i-1}}{N_c}, \quad (9)$$

$$a_{2i-1} = c_{2i-1} + \frac{c_{2i}}{N_c}. \quad (10)$$

N_c is the number of colors. The currents $j_\mu^q = \bar{q} \gamma_\mu (1 - \gamma_5) b$ and $J = \bar{c} (1 - \gamma_5) b$.

We have defined the decay constants of the pseudoscalar D_s meson and the vector D_s^* meson as

$$\langle D_s^-(p_{D_s}) | \bar{s} \gamma^\mu \gamma^5 c | 0 \rangle = i f_{D_s} p_{D_s}^\mu, \quad (11)$$

$$\langle D_s^{*-}(p_{D_s^*}, \epsilon) | \bar{s} \gamma_\mu c | 0 \rangle = m_{D_s^*} f_{D_s^*} \epsilon_\mu^{(\lambda)*}, \quad (12)$$

where ϵ stands for the polarization vector of the D_s^* meson. Using the definition (11) and the Dirac equation, it follows that

$$\langle D_s^- | \bar{s} (1 + \gamma_5) c | 0 \rangle = i f_{D_s} \frac{m_{D_s}^2}{m_c + m_s}, \quad (13)$$

which has been used to obtain Eq. (3).

III. INITIAL BOUND STATE EFFECT

In this section we study the initial b -quark bound state effect on $\bar{B} \rightarrow D_s^{(*)-} X_q$ using the light-cone expansion and the heavy quark effective theory. In the following we work out, in detail, the formulation for $\bar{B} \rightarrow D_s^- X_c$. The results for $\bar{B} \rightarrow D_s^{*-} X_c$ and $\bar{B} \rightarrow D_s^{(*)-} X_u$, which have a simpler structure in decay amplitudes, can be easily obtained along the same lines.

The differential decay rate for $\bar{B} \rightarrow D_s^- X_c$ in the \bar{B} rest frame is given by

$$d\Gamma(\bar{B} \rightarrow D_s^- X_c) = \frac{1}{2m_B} \frac{d^3 \mathbf{p}_{D_s}}{(2\pi)^3 2E_{D_s}} \sum_{X_c} (2\pi)^4 \delta^4(p_B - p_{D_s} - p_{X_c}) |A(\bar{B} \rightarrow D_s^- X_c)|^2. \quad (14)$$

Applying $\int d^4y \exp[-iy \cdot (p_B - p_{D_s} - p_{X_c})] = (2\pi)^4 \delta^4(p_B - p_{D_s} - p_{X_c})$, $\langle X_c | Q_\mu(0) | \bar{B} \rangle = \langle X_c | Q_\mu(y) | \bar{B} \rangle \exp[-iy \cdot (p_{X_c} - p_B)]$ due to translation invariance, and the completeness of the hadronic states $|X_c\rangle$, we obtain from Eq. (3)

$$\begin{aligned} & \sum_{X_c} (2\pi)^4 \delta^4(p_B - p_{D_s} - p_{X_c}) |A(\bar{B} \rightarrow D_s^- X_c)|^2 \\ &= f_{D_s}^2 \int d^4y e^{iy \cdot p_{D_s}} (|\alpha|^2 p_{D_s}^\mu p_{D_s}^\nu \langle \bar{B} | [j_\nu^{c\dagger}(0), j_\mu^c(y)] | \bar{B} \rangle + |\beta|^2 \langle \bar{B} | [J^\dagger(0), J(y)] | \bar{B} \rangle \\ &+ \alpha \beta^* p_{D_s}^\mu \langle \bar{B} | [J^\dagger(0), j_\mu^c(y)] | \bar{B} \rangle + \alpha^* \beta p_{D_s}^\mu \langle \bar{B} | [j_\mu^{c\dagger}(0), J(y)] | \bar{B} \rangle). \end{aligned} \quad (15)$$

Computing the commutators of currents yields

$$\begin{aligned} & \sum_{X_c} (2\pi)^4 \delta^4(p_B - p_{D_s} - p_{X_c}) |A(\bar{B} \rightarrow D_s^- X_c)|^2 \\ &= -2f_{D_s}^2 \left(|\alpha|^2 S_{\mu\alpha\nu\beta} p_{D_s}^\mu p_{D_s}^\nu + |\beta|^2 g_{\alpha\beta} \right) \int d^4y e^{iy \cdot p_{D_s}} [\partial^\alpha \Delta_c(y)] \langle \bar{B} | \bar{b}(0) \gamma^\beta U(0, y) b(y) | \bar{B} \rangle \\ &- 2f_{D_s}^2 (\alpha \beta^* + \alpha^* \beta) m_c p_{D_s}^\beta \int d^4y e^{iy \cdot p_{D_s}} i \Delta_c(y) \langle \bar{B} | \bar{b}(0) \gamma_\beta U(0, y) b(y) | \bar{B} \rangle, \end{aligned} \quad (16)$$

where $S_{\mu\alpha\nu\beta} = g_{\mu\alpha}g_{\nu\beta} + g_{\mu\beta}g_{\nu\alpha} - g_{\mu\nu}g_{\alpha\beta}$ and

$$\Delta_q(y) = -\frac{i}{(2\pi)^3} \int d^4k e^{-ik \cdot y} \varepsilon(k^0) \delta(k^2 - m_q^2). \quad (17)$$

The soft gluon interactions on the final state c quark appear in the Wilson line operator

$$U(x, y) = \mathcal{P} \exp [ig_s \int_y^x dz^\mu A_\mu(z)], \quad (18)$$

where \mathcal{P} denotes path-ordering and A^μ is the background gluon field. The initial bound state effect is contained in the matrix element of the non-local b -quark operator, $\langle \bar{B} | \bar{b}(0) \gamma^\beta U(0, y) b(y) | \bar{B} \rangle$. We note that the same matrix element also incorporates bound state effects in other inclusive B -meson decays, including $B \rightarrow \ell \bar{\nu}_\ell X_q$ [16], $B \rightarrow \gamma X_s$ [17], and $B \rightarrow K^{(*)} X$ [18]. We shall use the light-cone expansion to calculate the matrix element. The light-cone expansion enables a systematic ordering of nonperturbative QCD effects as an expansion in powers of a small parameter of order $\Lambda_{\text{QCD}}^2/m_B^2$. The general method has been described in [16,17]. We shall restrict ourselves here to the essential steps only.

Each integrand of the integrals in Eq. (16) contains an oscillating factor $e^{iy \cdot p_{D_s}}$. The dominant contribution comes from domains with less rapid oscillations, i.e., $|y \cdot p_{D_s}| \sim 1$. This implies that for sufficiently large momentum of the outgoing D_s meson, the decay dynamics is dominated by spacetime separations in the neighborhood of the light cone $y^2 = 0$. The light-cone dominance is also justified since the function $\Delta_c(y)$ in the integrals in Eq. (16) has a singularity at $y^2 = 0$. Therefore, at leading twist we have²

²Higher twist effects have been analyzed quantitatively in [19]. They give rise to corrections of order $\Lambda_{\text{QCD}}^2/m_B^2$ and can be added systematically. The calculation of higher twist effects on the processes under consideration is beyond the scope of this paper.

$$\langle \bar{B} | \bar{b}(0) \gamma^\beta U(0, y) b(y) | \bar{B} \rangle = 2p_B^\beta \int_0^1 d\xi e^{-i\xi y \cdot p_B} f(\xi), \quad (19)$$

where $f(\xi)$ is the b -quark distribution function of the B meson introduced in Refs. [16,17]

$$f(\xi) = \frac{1}{4\pi} \int \frac{d(y \cdot p_B)}{y \cdot p_B} e^{i\xi y \cdot p_B} \langle \bar{B} | \bar{b}(0) y U(0, y) b(y) | \bar{B} \rangle |_{y^2=0}. \quad (20)$$

Note that $f(\xi)$ depends only on the properties of the B -meson bound state and is not specific to particular B -meson decay process in question. Thus, $f(\xi)$ is a universal distribution as fundamental as parton distributions in deep inelastic scattering. It has the interpretation of the probability of finding a b -quark with momentum ξp_B inside the B meson with momentum p_B [17,20].

Assembling all the pieces, we obtain the momentum spectrum for D_s^- in $\bar{B} \rightarrow D_s^- X_c$

$$\begin{aligned} \frac{d\Gamma}{d|\mathbf{p}_{D_s}|}(\bar{B} \rightarrow D_s^- X_c) = & \frac{f_{D_s}^2}{\pi} \frac{|\mathbf{p}_{D_s}|^2}{E_{D_s}} \int_0^1 d\xi f(\xi) \varepsilon(E_{D_s} - m_B \xi) \\ & \times \delta(m_B^2 \xi^2 - 2m_B E_{D_s} \xi + m_{D_s}^2 - m_c^2) \\ & \times [|\alpha|^2 (m_{D_s}^2 E_{D_s} + m_B m_{D_s}^2 \xi - 2m_B E_{D_s}^2 \xi) + |\beta|^2 (E_{D_s} - m_B \xi) \\ & - (\alpha \beta^* + \alpha^* \beta) m_c E_{D_s}]. \end{aligned} \quad (21)$$

Carrying out the δ -function integration in Eq. (21), we finally arrive at

$$\begin{aligned} \frac{d\Gamma}{d|\mathbf{p}_{D_s}|}(\bar{B} \rightarrow D_s^- X_c) = & \frac{f_{D_s}^2}{2\pi m_B} \frac{|\mathbf{p}_{D_s}|^2}{E_{D_s} \sqrt{|\mathbf{p}_{D_s}|^2 + m_c^2}} \\ & \times \{ f(\xi_+^c) [|\alpha|^2 (2m_B E_{D_s}^2 \xi_+^c - m_B m_{D_s}^2 \xi_+^c - m_{D_s}^2 E_{D_s}) \\ & + |\beta|^2 (m_B \xi_+^c - E_{D_s}) + (\alpha \beta^* + \alpha^* \beta) m_c E_{D_s}] \\ & - (\xi_+^c \rightarrow \xi_-^c) \}, \end{aligned} \quad (22)$$

where

$$\xi_\pm^q = \frac{E_{D_s} \pm \sqrt{|\mathbf{p}_{D_s}|^2 + m_q^2}}{m_B}. \quad (23)$$

The interference between the tree and penguin amplitudes is associated with the coefficients $|\alpha|^2$ and $\alpha \beta^* + \alpha^* \beta$.

In the case of the $\bar{B} \rightarrow D_s^{*-} X_c$ and $\bar{B} \rightarrow D_s^{(*)-} X_u$ decays, similar considerations lead to the momentum spectra in the \bar{B} rest frame

$$\begin{aligned} \frac{d\Gamma}{d|\mathbf{p}_{D_s^*}|}(\bar{B} \rightarrow D_s^{*-} X_c) = & \frac{f_{D_s^*}^2}{2\pi m_B} |\alpha|^2 \frac{|\mathbf{p}_{D_s^*}|^2}{E_{D_s^*} \sqrt{|\mathbf{p}_{D_s^*}|^2 + m_c^2}} \\ & \times \left[f(\xi_+^{*c}) \left(2m_B E_{D_s^*}^2 \xi_+^{*c} + m_B m_{D_s^*}^2 \xi_+^{*c} - 3m_{D_s^*}^2 E_{D_s^*} \right) - (\xi_+^{*c} \rightarrow \xi_-^{*c}) \right], \quad (24) \\ \frac{d\Gamma}{d|\mathbf{p}_{D_s}|}(\bar{B} \rightarrow D_s^- X_u) = & \frac{G_F^2}{4\pi m_B} |V_{ub} V_{cs}^*|^2 a_1^2 f_{D_s}^2 \frac{|\mathbf{p}_{D_s}|^2}{E_{D_s} \sqrt{|\mathbf{p}_{D_s}|^2 + m_u^2}} \end{aligned}$$

$$\times \left[f(\xi_+^u) \left(2m_B E_{D_s}^2 \xi_+^u - m_B m_{D_s}^2 \xi_+^u - m_{D_s}^2 E_{D_s} \right) - \left(\xi_+^u \rightarrow \xi_-^u \right) \right], \quad (25)$$

$$\begin{aligned} \frac{d\Gamma}{d|\mathbf{p}_{D_s^*}|}(\bar{B} \rightarrow D_s^{*-} X_u) &= \frac{G_F^2}{4\pi m_B} |V_{ub} V_{cs}|^2 a_1^2 f_{D_s^*}^2 \frac{|\mathbf{p}_{D_s^*}|^2}{E_{D_s^*} \sqrt{|\mathbf{p}_{D_s^*}|^2 + m_u^2}} \\ &\times \left[f(\xi_+^{*u}) \left(2m_B E_{D_s^*}^2 \xi_+^{*u} + m_B m_{D_s^*}^2 \xi_+^{*u} - 3m_{D_s^*}^2 E_{D_s^*} \right) - \left(\xi_+^{*u} \rightarrow \xi_-^{*u} \right) \right], \quad (26) \end{aligned}$$

where

$$\xi_{\pm}^{*q} = \frac{E_{D_s^*} \pm \sqrt{|\mathbf{p}_{D_s^*}|^2 + m_q^2}}{m_B}. \quad (27)$$

For a longitudinally polarized D_s^{*-} we obtain

$$\begin{aligned} \frac{d\Gamma_L}{d|\mathbf{p}_{D_s^*}|}[\bar{B} \rightarrow D_s^{*-}(\lambda = 0) X_c] &= \frac{f_{D_s^*}^2}{2\pi m_B} |\alpha|^2 \frac{|\mathbf{p}_{D_s^*}|^2}{E_{D_s^*} \sqrt{|\mathbf{p}_{D_s^*}|^2 + m_c^2}} \\ &\times \left[f(\xi_+^{*c}) \left(2m_B |\mathbf{p}_{D_s^*}|^2 \xi_+^{*c} + m_B m_{D_s^*}^2 \xi_+^{*c} - m_{D_s^*}^2 E_{D_s^*} \right) - \left(\xi_+^{*c} \rightarrow \xi_-^{*c} \right) \right]. \quad (28) \end{aligned}$$

For a transversely polarized D_s^{*-} we have

$$\begin{aligned} \frac{d\Gamma_T}{d|\mathbf{p}_{D_s^*}|}[\bar{B} \rightarrow D_s^{*-}(\lambda = \pm 1) X_c] &= \frac{m_{D_s^*}^2 f_{D_s^*}^2}{\pi m_B} |\alpha|^2 \frac{|\mathbf{p}_{D_s^*}|^2}{E_{D_s^*} \sqrt{|\mathbf{p}_{D_s^*}|^2 + m_c^2}} \left[f(\xi_+^{*c}) \left(m_B \xi_+^{*c} - E_{D_s^*} \right) - \left(\xi_+^{*c} \rightarrow \xi_-^{*c} \right) \right]. \quad (29) \end{aligned}$$

From Eq. (22) one can easily obtain the hadronic invariant mass spectrum for X_c in $\bar{B} \rightarrow D_s^- X_c$ using the relation

$$\frac{d\Gamma}{dm_{X_c}}(\bar{B} \rightarrow D_s^- X_c) = \frac{m_{X_c} E_{D_s}}{m_B |\mathbf{p}_{D_s}|} \frac{d\Gamma}{d|\mathbf{p}_{D_s}|}(\bar{B} \rightarrow D_s^- X_c). \quad (30)$$

Similar formulas hold for the hadronic invariant mass spectra in $\bar{B} \rightarrow D_s^{*-} X_c$ and $\bar{B} \rightarrow D_s^{(*)-} X_u$.

The total decay rates can be obtained by integrating Eqs. (22), (24)-(26), (28) and (29) with respect to $|\mathbf{p}_{D_s^{(*)}}|$ over the entire kinematic range

$$0 \leq |\mathbf{p}_{D_s^{(*)}}| \leq \sqrt{[(m_B + m_{D_s^{(*)}})^2 - m_{X_{q_{\min}}}^2][(m_B - m_{D_s^{(*)}})^2 - m_{X_{q_{\min}}}^2]} / (2m_B), \quad (31)$$

where $m_{X_{q_{\min}}}$ is the minimum value of the invariant mass of the hadronic system X_q .

Measurements of the ratio of the decay rate for the longitudinally polarized D_s^{*-} to the total decay rate for $\bar{B} \rightarrow D_s^{*-} X_c$ have a good potential for testing the theory, since the theoretical uncertainties partly cancel in the ratio and most of experimental systematic errors also cancel.

The leading effect of the initial B bound state is encoded in the distribution function $f(\xi)$. Since it is a nonperturbative QCD object, $f(\xi)$ has not yet been completely determined. Nevertheless, several important properties of it are known in QCD [16,17]. The distribution function is exactly normalized to unity, $\int_0^1 d\xi f(\xi) = 1$, because of the conservation of the b -quark vector current by the strong interactions. For a free b -quark, $b(y) = e^{-iy \cdot p_b} b(0)$. From Eq. (20) it follows then that in the free quark limit

$$f_{\text{free}}(\xi) = \delta\left(\xi - \frac{m_b}{m_B}\right). \quad (32)$$

The mean $\langle \xi \rangle = \int_0^1 d\xi \xi f(\xi)$ and the variance $\sigma^2 = \langle (\xi - \langle \xi \rangle)^2 \rangle = \int_0^1 d\xi (\xi - \langle \xi \rangle)^2 f(\xi)$ characterize the location of the “center of mass” of the distribution function and the square of its width, respectively. They specify the gross shape of the distribution function. They have been estimated using the heavy quark effective theory. The results are [16,17]

$$\langle \xi \rangle = \frac{m_b}{m_B} \left[1 - \frac{5}{6m_b^2} (\lambda_1 + 3\lambda_2) \right], \quad (33)$$

$$\sigma^2 = -\frac{\lambda_1}{3m_B^2}, \quad (34)$$

where λ_1 and λ_2 are the HQET parameters, which are defined as

$$\lambda_1 = \frac{1}{2m_B} \langle \bar{B} | \bar{h}_v (iD)^2 h_v | \bar{B} \rangle, \quad (35)$$

$$\lambda_2 = \frac{1}{12m_B} \langle \bar{B} | \bar{h}_v g_s G_{\mu\nu} \sigma^{\mu\nu} h_v | \bar{B} \rangle. \quad (36)$$

Both of them are expected to be of order Λ_{QCD}^2 . These imply that the distribution function is sharply peaked around m_b/m_B with a width of order Λ_{QCD}/m_B . This is in line with the expectation that the b quark should carry most of the momentum of the B meson.

Another important property of the distribution function, discussed previously, is universality. This implies that the distribution function can be extracted from measurements of one process, and then applied to predict others in a model-independent way. Indeed, the shape of the distribution function can be directly extracted from $B \rightarrow \ell \bar{\nu}_\ell X_q$ [21] or $B \rightarrow \gamma X_s$ [17] decays. This could eventually improve the precision of theoretical predictions.

For numerical analyses we take the following parameterization for the distribution function [22]

$$f(\xi) = N \frac{\xi(1-\xi)^c}{[(\xi-a)^2 + b^2]^d}, \quad (37)$$

where N is a normalization constant which guarantees $\int_0^1 d\xi f(\xi) = 1$. The four shape parameters, (a, b, c, d) , obey all the known constraints on the distribution function. Once the parameters c and d are given, the parameters a and b can be fixed by comparing with $\langle \xi \rangle$ and σ^2 given in Eqs. (33) and (34). Unfortunately, we do not know the values for c and d at present. We shall take c and d to be free parameters and vary them to gain an idea of how the momentum spectra for $D_s^{(*)}$ and branching fractions depend on the shape of $f(\xi)$. Eventually, the shape of the distribution function can be determined from experimental data. The parameterization (37) facilitates the comparison to data.

IV. FREE QUARK LIMIT

In order to understand the bound state dynamics of the B meson in the semi-inclusive B meson decays, we should consider the decay rates for the free quark decays, $b \rightarrow D_s^{(*)-} q$, which give us a reference point.

In the free quark limit, the distribution function becomes a δ -function. Substituting the free b -quark distribution function Eq. (32) in Eqs. (22) [or, most easily, Eq. (21)] and (24)-(26), we reproduce the corresponding total decay rates for the free quark decays in the rest frame of the b quark:

$$\begin{aligned} \Gamma(b \rightarrow D_s^- c) &= \frac{f_{D_s}^2}{4\pi m_b^2} |\mathbf{p}_{D_s}| \{ |\alpha|^2 [(m_b^2 - m_c^2)^2 - m_{D_s}^2(m_b^2 + m_c^2)] + |\beta|^2 (m_b^2 + m_c^2 - m_{D_s}^2) \\ &\quad + (\alpha\beta^* + \alpha^*\beta) m_c(m_b^2 - m_c^2 + m_{D_s}^2) \}, \end{aligned} \quad (38)$$

$$\Gamma(b \rightarrow D_s^{*-} c) = \frac{f_{D_s^*}^2}{4\pi m_b^2} |\alpha|^2 |\mathbf{p}_{D_s^*}| [(m_b^2 - m_c^2)^2 + m_{D_s^*}^2(m_b^2 + m_c^2 - 2m_{D_s^*}^2)], \quad (39)$$

$$\Gamma(b \rightarrow D_s^- u) = \frac{G_F^2}{8\pi m_b^2} |V_{ub} V_{cs}^*|^2 a_1^2 f_{D_s}^2 |\mathbf{p}_{D_s}| [(m_b^2 - m_u^2)^2 - m_{D_s}^2(m_b^2 + m_u^2)], \quad (40)$$

$$\Gamma(b \rightarrow D_s^{*-} u) = \frac{G_F^2}{8\pi m_b^2} |V_{ub} V_{cs}^*|^2 a_1^2 f_{D_s^*}^2 |\mathbf{p}_{D_s^*}| [(m_b^2 - m_u^2)^2 + m_{D_s^*}^2(m_b^2 + m_u^2 - 2m_{D_s^*}^2)]. \quad (41)$$

Similarly, substituting Eq. (32) in Eqs. (28) and (29), we reproduce the corresponding decay rates for $b \rightarrow D_s^{*-} c$ with the longitudinal and transverse polarizations of D_s^{*-} , respectively,

$$\Gamma_L[b \rightarrow D_s^{*-}(\lambda=0)c] = \frac{f_{D_s^*}^2}{4\pi m_b^2} |\alpha|^2 |\mathbf{p}_{D_s^*}| [(m_b^2 - m_c^2)^2 - m_{D_s^*}^2(m_b^2 + m_c^2)], \quad (42)$$

$$\Gamma_T[b \rightarrow D_s^{*-}(\lambda=\pm 1)c] = \frac{m_{D_s^*}^2 f_{D_s^*}^2}{2\pi m_b^2} |\alpha|^2 |\mathbf{p}_{D_s^*}| (m_b^2 + m_c^2 - m_{D_s^*}^2). \quad (43)$$

It follows from Eqs. (39) and (42) that the ratio of the decay rate for the longitudinally polarized D_s^{*-} to the total decay rate for $b \rightarrow D_s^{*-} c$

$$\frac{\Gamma_L}{\Gamma}(b \rightarrow D_s^{*-} c) = 1 - \frac{2m_{D_s^*}^2(m_b^2 + m_c^2 - m_{D_s^*}^2)}{(m_b^2 - m_c^2)^2 + m_{D_s^*}^2(m_b^2 + m_c^2 - 2m_{D_s^*}^2)}. \quad (44)$$

Our results for the part of the free quark decay rate involving tree diagrams agree with Refs. [1,2]. It should be stressed that the reproduction of the free quark decay results by taking the free quark limit of the leading twist results shows consistency of the light-cone expansion.

All the momentum spectra for $D_s^{(*)-}$ in the free quark decays $b \rightarrow D_s^{(*)-} q$ are a discrete line localized at

$$|\mathbf{p}_{D_s^{(*)}}| = \sqrt{[(m_b + m_{D_s^{(*)}})^2 - m_q^2][(m_b - m_{D_s^{(*)}})^2 - m_q^2]} / (2m_b) \quad (45)$$

because the momentum of $D_s^{(*)-}$ in the two-body decay is fixed kinematically.

As shown in the last section, at the hadron level the momentum spectrum for $D_s^{(*)-}$ in $\bar{B} \rightarrow D_s^{(*)-} X_q$ spreads over the kinematic range given in Eq. (31), due to the fact that the hadronic invariant mass m_{X_q} is changeable. However, since the heavy b quark in the B meson is nearly free, most of the spectrum remain around the free quark decay location of (45). This is the phase space region where light-cone dominance occurs.

For measurements of $\bar{B} \rightarrow D_s^{(*)-} X_u$ one can apply the cut on the $D_s^{(*)-}$ momentum above the limit for charm production in the decay, $|\mathbf{p}_{D_s^{(*)}}| > \sqrt{[(m_B + m_{D_s^{(*)}})^2 - m_D^2][(m_B - m_{D_s^{(*)}})^2 - m_D^2]} / (2m_B)$, to suppress the $\bar{B} \rightarrow D_s^{(*)-} X_c$ background. Since this cut is well below the free quark decay location of (45), the majority of the momentum spectrum in $\bar{B} \rightarrow D_s^{(*)-} X_u$ pass the cut, as we shall see.

V. NUMERICAL ANALYSES

For numerical analyses, we must specify the values of the input parameters. We use $G_F = 1.16639 \times 10^{-5}$ GeV $^{-2}$, $m_B = 5.279$ GeV, $m_{D_s} = 1.969$ GeV, $m_{D_s^*} = 2.112$ GeV, $m_D = 1.87$ GeV, and $m_\pi = 0$. We neglect the B^+ , B^0 lifetime difference and use $\tau_B = 1.6 \times 10^{-12}$ sec. For quark masses, we use $m_b = 4.9$ GeV, $m_c = 1.5$ GeV, $m_s = 120$ MeV, and $m_u = 0$. As for the CKM matrix elements, we take $|V_{ub}| = 0.0035$, $|V_{cs}| = 0.9742$, $|V_{cb}| = |V_{ts}| = 0.04$, and $|V_{tb}| = 0.9992$. Since the phase $\omega_{ud} \equiv \arg(-V_{cs}^* V_{tb}^* V_{cb} V_{ts})$ is very small, we assume $\cos \omega_{ud} = 1$. For the decay constants, we take $f_{D_s} = 264$ MeV from the measurements of the leptonic branching fractions $\text{Br}(D_s \rightarrow \tau \nu)$ and $\text{Br}(D_s \rightarrow \mu \nu)$ [23] and assume $f_{D_s^*} = f_{D_s}$. We take $m_{X_{c_{\min}}} = m_c$ for $\bar{B} \rightarrow D_s^{(*)-} X_c$ and $m_{X_{u_{\min}}} = 0$ for $\bar{B} \rightarrow D_s^{(*)-} X_u$. Finally, we consider two very different shapes of the distribution function parameterized in Eq. (37), corresponding to two sets of parameters: (i) preset $c = d = 1$, in that case $a = 0.9548$ and $b = 0.005444$, which are inferred from the known mean value and variance of the distribution function given by Eqs. (33) and (34) using the HQET parameters $\lambda_1 = -0.5$ GeV 2 and $\lambda_2 = 0.12$ GeV 2 ; (ii) preset $c = d = 2$, in that case $a = 0.9864$ and $b = 0.02557$ inferred from the same mean value and variance of the distribution function [22].

We first compute the branching fractions for $\bar{B} \rightarrow D_s^{(*)-} X_q$. It turns out that the branching fractions are not sensitive to the detailed shape of the distribution function. The difference between the branching fractions obtained using the parameter sets (i) and (ii) for the distribution function is negligible. The results for the direct production of $D_s^{(*)-}$ in semi-inclusive B decays are

$$\begin{aligned} \mathcal{B}(\bar{B} \rightarrow D_s^- X_c) &= 4.0\%, \\ \mathcal{B}(\bar{B} \rightarrow D_s^{*-} X_c) &= 5.4\%, \\ \mathcal{B}(\bar{B} \rightarrow D_s^- X_u) &= 4.8 \times 10^{-4}, \\ \mathcal{B}(\bar{B} \rightarrow D_s^{*-} X_u) &= 6.2 \times 10^{-4}. \end{aligned} \tag{46}$$

The calculated branching fraction for $\bar{B} \rightarrow D_s^{*-} X_c$ is in agreement with the measured one by BABAR quoted in the Introduction. Because D_s^{*-} decays to $D_s^- \gamma$ or $D_s^- \pi^0$, we can compare the sum of both channels, $\mathcal{B}(\bar{B} \rightarrow D_s^- X_c) + \mathcal{B}(\bar{B} \rightarrow D_s^{*-} X_c) = 9.4\%$, from Eq. (46) with the

measured branching fraction for $B \rightarrow D_s^\pm X$ quoted in the Introduction. The comparison shows an encouraging agreement.

We find that the contribution of the penguin amplitude decreases the branching fraction for $\bar{B} \rightarrow D_s^- X_c$ by 3% and the branching fraction for $\bar{B} \rightarrow D_s^{*-} X_c$ by 6%. So the penguin contribution is small but non-negligible, especially for $\bar{B} \rightarrow D_s^{*-} X_c$.

Comparing with the calculations in the free quark decays $b \rightarrow D_s^{(*)-} q$, we find that all the branching fractions for $\bar{B} \rightarrow D_s^{(*)-} X_q$ are enhanced by the initial bound state effect by about 5%.

The ratio of the decay rate for the longitudinally polarized D_s^{*-} to the total decay rate for $\bar{B} \rightarrow D_s^{*-} X_c$ is also insensitive to the detailed shape of the distribution function. The bound state effect increases the ratio by 2% compared to the free quark decay. We obtain

$$\frac{\Gamma_L}{\Gamma}(\bar{B} \rightarrow D_s^{*-} X_c) = 0.66. \quad (47)$$

Now we turn to the differential decay rates. Figures 1-4 show the momentum spectra for $D_s^{(*)-}$ in $\bar{B} \rightarrow D_s^{(*)-} X_q$. We choose to use two very different shapes of the distribution function to calculate the spectra. In contrast to the integrated decay rates, all the spectra depend strongly on the shape of the distribution function. Hence measurements of the spectra can provide useful information about the nonperturbative distribution function.

As Figs. 3 and 4 make clear, the majority of the momentum spectrum for $D_s^{(*)-}$ in the decay mode $\bar{B} \rightarrow D_s^{(*)-} X_u$ lie above the kinematic limit for the dominated decay mode $\bar{B} \rightarrow D_s^{*-} X_c$, which is $|\mathbf{p}_{D_s}| > 1.81$ GeV for $\bar{B} \rightarrow D_s^- X_u$ and $|\mathbf{p}_{D_s^*}| > 1.73$ GeV for $\bar{B} \rightarrow D_s^{*-} X_u$. The fraction of spectrum above the charmed limit is not sensitive to the shape of the distribution function. We find that about 98% of the spectrum goes beyond the charmed limit. Thus, the kinematic cut on the momentum of $D_s^{(*)}$ provides an efficient discrimination between $\bar{B} \rightarrow D_s^{(*)-} X_u$ decays and $\bar{B} \rightarrow D_s^{(*)-} X_c$ decays.

VI. DISCUSSION AND CONCLUSION

We have calculated the total and differential $\bar{B} \rightarrow D_s^{(*)-} X_q$ decay rates assuming factorization. We have treated the initial bound state effect using the light-cone expansion and the heavy quark effective theory, generating a theoretical description of this effect from QCD rather than the phenomenological model [2]. The resulting branching fractions for $\bar{B} \rightarrow D_s^{(*)-} X_c$ are found to be in agreement with the measurements. This suggests that factorization is a fair approximation for these decay modes. However, there are still considerable uncertainties in the theoretical calculations and experimental measurements. Theoretical uncertainties arise from the input parameters, the b -quark distribution function, the higher twist corrections, and the radiative corrections. The uncertainty in the decay rate from the error on the decay constant f_{D_s} alone [23] is already quite large ($\sim 30\%$).

For the determination of $|V_{ub}|$ from $\bar{B} \rightarrow D_s^{(*)-} X_u$, additional theoretical uncertainty results from the underlying factorization hypothesis itself. It is hard to quantify this uncertainty. Therefore, $|V_{ub}|$ determined from the semi-inclusive nonleptonic decay $B \rightarrow D_s^{(*)-} X_u$ will not be competitive with that determined from the inclusive semileptonic decay $\bar{B} \rightarrow \ell \bar{\nu}_\ell X_u$ [24]. Nevertheless, $\bar{B} \rightarrow D_s^{(*)-} X_u$ will provide a useful independent measurement of

$|V_{ub}|$ with very different systematic errors. On the other hand, using $|V_{ub}|$ determined from the inclusive semileptonic B decay, the range of validity of calculational tools for addressing QCD can be tested and established in $\bar{B} \rightarrow D_s^{(*)-} X_u$,

ACKNOWLEDGMENTS

It is a pleasure to thank Berthold Stech for useful discussions. This work is supported by the Australian Research Council.

REFERENCES

- [1] W.F. Palmer and B. Stech, Phys. Rev. D **48**, 4174 (1993).
- [2] R. Aleksan *et al.*, Phys. Rev. D **62**, 093017 (2000).
- [3] Y. Koide, Phys. Rev. D **39**, 3500 (1989);
 D. Choudhury, D. Indumati, A. Soni, and S.U. Sankar, Phys. Rev. D **45**, 217 (1992);
 I. Dunietz and J.L. Rosner, CERN-TH-5899-90;
 D.S. Du and C. Liu, Phys. Rev. D **50**, 4558 (1994);
 M. Beneke, G. Buchalla, and I. Dunietz, Phys. Lett. B **393**, 132 (1997);
 A.F. Falk and A.A. Petrov, Phys. Rev. D **61**, 033003 (2000);
 J. Chay *et al.*, Phys. Rev. D **61**, 034020 (2000);
 C.S. Kim, Y. Kwon, J. Lee, and W. Namgung, Phys. Rev. D **63**, 094506 (2001);
 C.S. Kim *et al.*, hep-ph/0203093.
- [4] Particle Data Group, D.E. Groom *et al.*, Eur. Phys. J. C **15**, 1 (2000).
- [5] BABAR Collaboration, B. Aubert *et al.*, hep-ex/0201041.
- [6] For a review, see G. Buchalla, A. Buras, and M. Lautenbacher, Rev. Mod. Phys. **68**, 1125 (1996).
- [7] K.G. Wilson, Phys. Rev. **179**, 1499 (1969);
 W. Zimmermann, *Lectures on Elementary Particles and Quantum Field Theory*, Brandeis Summer Institute (1970) Vol.1 (MIT Press, Cambridge, MA, 1970).
- [8] E.C.G. Stueckelberg and A. Peterman, Helv. Phys. Acta **24**, 317 (1951); **26**, 499 (1953);
 M. Gell-Mann and F.E. Low, Phys. Rev. **95**, 1300 (1954);
 N.N. Bogoliubov and D.V. Shirkov, Nuovo Cim. **3**, 845 (1956);
 C. Callan Jr., Phys. Rev. D **2**, 1541 (1970);
 K. Symanzik, Commun. Math. Phys. **18**, 227 (1970); **23**, 49 (1971).
- [9] M. Bauer and B. Stech, Phys. Lett. B **152**, 380 (1985);
 M. Bauer, B. Stech, and M. Wirbel, Z. Phys. C **34**, 103 (1987);
 M. Neubert and B. Stech, in *Heavy Flavours II*, edited by A.J. Buras and M. Lindner (World Scientific, Singapore, 1998), p.294, hep-ph/9705292.
- [10] J.D. Bjorken, Nucl. Phys. B (Proc. Suppl.) **11**, 325 (1989).
- [11] C.H. Chang and H.-n. Li, Phys. Rev. D **55**, 5577 (1997);
 T.W. Yeh and H.-n. Li, Phys. Rev. D **56**, 1615 (1997);
 H.Y. Cheng, H.-n. Li, and K.C. Yang, Phys. Rev. D **60**, 094005 (1999);
 Y.Y. Keum, H.-n. Li, and A.I. Sanda, Phys. Lett. B **504**, 6 (2001); Phys. Rev. D **63**, 054008 (2001);
 Y.Y. Keum and H.-n. Li, Phys. Rev. D **63**, 074006 (2001);
 C.D. Lü, K. Ukai, and M.Z. Yang, Phys. Rev. D **63**, 074009 (2001);
 C.H. Chen and H.-n. Li, Phys. Rev. D **63**, 014003 (2001);
 H.-n. Li, Phys. Rev. D **64**, 014019 (2001).
- [12] M. Beneke, G. Buchalla, M. Neubert, and C.T. Sachrajda, Phys. Rev. Lett. **83**, 1914 (1999); Nucl. Phys. B **591**, 313 (2000); Nucl. Phys. B **606**, 245 (2001).
- [13] C.W. Bauer, D. Pirjol, and I.W. Stewart, Phys. Rev. Lett. **87**, 201806 (2001).
- [14] Z. Luo and J.L. Rosner, Phys. Rev. D **64**, 094001 (2001).
- [15] N. Isgur and M.B. Wise, Phys. Lett. B **232**, 113 (1989); **237**, 527 (1990);

E. Eichten and B. Hill, Phys. Lett. B **234**, 511 (1990); **243**, 427 (1990);
 H. Georgi, Phys. Lett. B **240**, 447 (1990).

[16] C.H. Jin and E.A. Paschos, in *Proceedings of the International Symposium on Heavy Flavor and Electroweak Theory*, Beijing, China, 1995, edited by C.H. Chang and C.S. Huang (World Scientific, Singapore, 1996), p. 132; hep-ph/9504375;
 C.H. Jin, Phys. Rev. D **56**, 2928 (1997);
 C.H. Jin and E.A. Paschos, Eur. Phys. J. C **1**, 523 (1998);
 C.H. Jin, Phys. Rev. D **56**, 7267 (1997).

[17] C.H. Jin, Eur. Phys. J. C **11**, 335 (1999).

[18] X.-G. He, C.H. Jin, and J.P. Ma, Phys. Rev. D **64**, 014020 (2001).

[19] C.H. Jin, Phys. Lett. B **520**, 92 (2001).

[20] A. Bareiss and E.A. Paschos, Nucl. Phys. B **327**, 353 (1989);
 C.H. Jin, W.F. Palmer, and E.A. Paschos, Phys. Lett. B **329**, 364 (1994).

[21] C.H. Jin, Mod. Phys. Lett. A **14**, 1163 (1999); Phys. Rev. D **62**, 014020 (2000).

[22] C.H. Jin, Phys. Rev. D **57**, 6851 (1998).

[23] S. Söldner-Rembold, hep-ex/0109023.

[24] For a recent review, see C.H. Jin, Theory of Extracting $|V_{cb}|$ and $|V_{ub}|$, talk given at the 18th International Workshop on Weak Interactions and Neutrinos, Christchurch, New Zealand, 21-26 Jan. 2002, <http://www.anta.canterbury.ac.nz/neutrino/>.

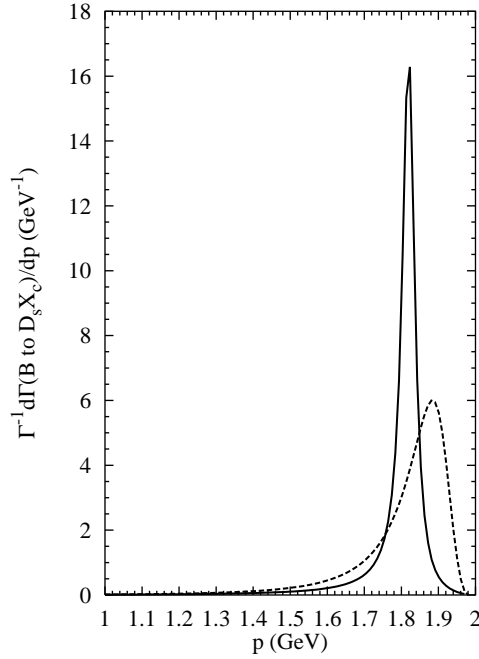


FIG. 1. Momentum spectrum for D_s^- in $\bar{B} \rightarrow D_s^- X_c$. In Figs. 1-4, the solid curves are obtained using the parameter set (i) for the distribution function; the dashed curves are obtained using the parameter set (ii) for the distribution function.

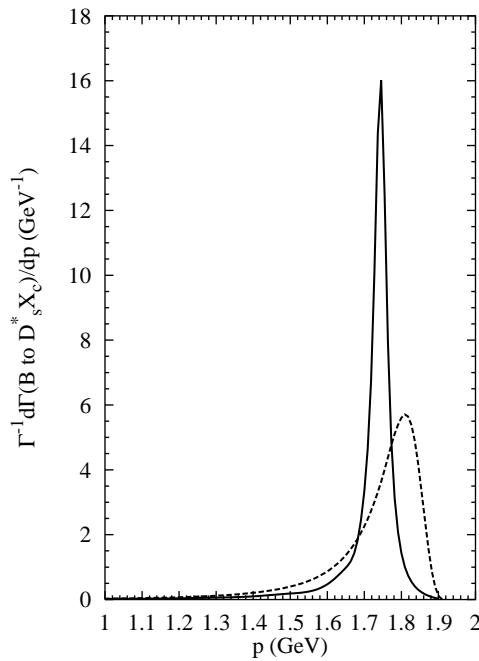


FIG. 2. Momentum spectrum for D_s^{*-} in $\bar{B} \rightarrow D_s^{*-} X_c$.

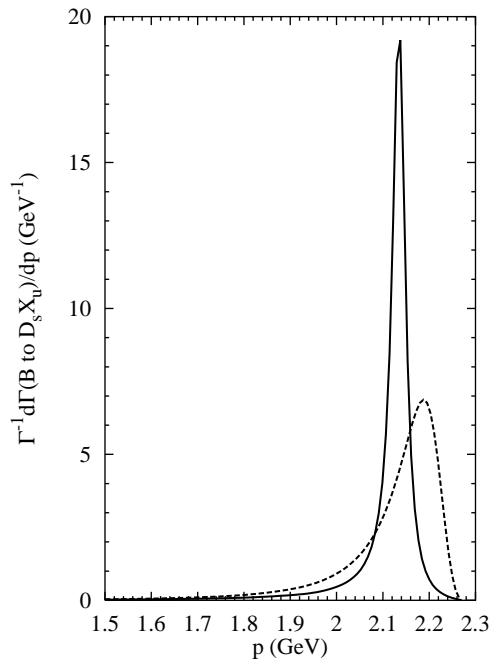


FIG. 3. Momentum spectrum for D_s^- in $\bar{B} \rightarrow D_s^- X_u$.

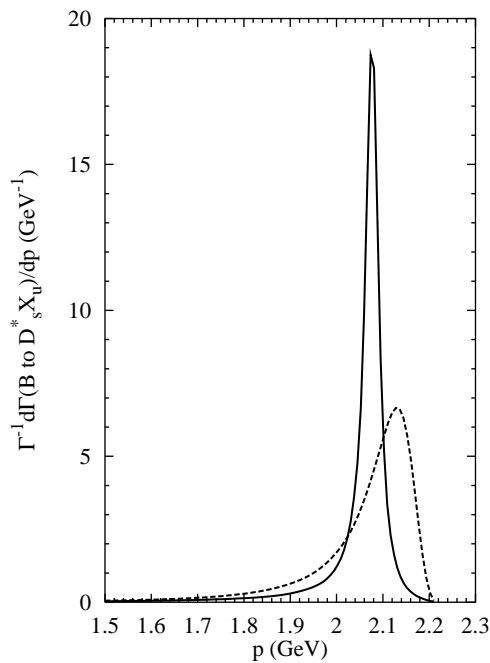


FIG. 4. Momentum spectrum for D_s^{*-} in $\bar{B} \rightarrow D_s^{*-} X_u$.